

# Event-Based Under-Frequency Inertia Emulation Scheme for Severe Conditions

Mojtaba Eliassi<sup>\*</sup>, Pedro A. Betancourt Paulino<sup>\*</sup>, Roozbeh Torkzadeh<sup>\*</sup>, Pedro Rodriguez<sup>\*†</sup>

<sup>\*</sup>Research Institute of Science and Technology (Loyola Tech.),  
Loyola University Andalusia, Seville, Spain.

<sup>†</sup>Research center on Renewable Electrical Energy Systems (SEER),  
Technical University of Catalonia, Barcelona, Spain.

Email: {meliassi, pabetancourt, rtorkzadeh, prodriguez}@uloyola.es  
prodriguez@ee.upc.edu

**Abstract**— The existing UFLS schemes suggested for conventional power systems need to be reassessed in the presence of renewable energy sources and storage systems equipped with grid-supporting convertors. A new Event-Based Under-Frequency Inertia Emulation (EB-UFIE) plan is proposed in this paper as a substitute of traditional UFLS program to protect the system against the risk of generation trip and subsequent blackout. Trajectory sensitivities are used as a popular technique to predict the future behavior of the system through a mixed integer programming optimization problem. The proposed scheme has been tested on the modified New England 39-bus system including renewables and storages.

**Keywords**— *Under-Frequency Load Shedding; Inertia Emulation; Distributed Energy Resources; Fast-response Storages; Mixed Integer Programming; Trajectory Sensitives, ROCOF.*

## I. INTRODUCTION

A rising interest to investigate the impact of high penetration of renewable generation on frequency control of power system and the capability of delivering frequency support by renewables is emerged during recent years [1]. Although, decrease of system inertia and conventional spinning reserve and increase of uncertainties by integrating renewables in the generation mix deteriorates the frequency support, but by implementation of virtual synchronous machine behavior [2]-[3] through the new grid-supporting convertors of storages and renewables, the frequency support can be improved by means of the provided fast synthetic inertia and timely generation control in severe conditions [4].

In severe frequency decline situations, Under-Frequency Load Shedding (UFLS) programs (generally including event-based and response-based UFLSs) used to be the only appropriate way and last automated measure to prevent a power system from collapsing, designed and implemented by Transmission System Operator (TSO) through dynamic off-line simulations in operational planning time-scale. In response-based UFLS programs, the relay settings are usually pre-defined, fixed, and non-robust which may not be a comprehensive solution for the wide range of combinational/cascading events [5]. Event-based plans are more reliable and secure in case of

high consequence events because of its immediate reaction to predefined events, rather than waiting for a fixed threshold of frequency and time delay.

The UFLS as a traditional emergency control action has not been investigated enough under high share of renewable energy sources. The existing UFLS schemes suggested for conventional power systems need to be reassessed in the presence of renewable energy sources and storage systems equipped with grid-supporting convertors. Although the effect of fast acting power controller of Energy Storage Systems (EESs) on UFLS and mal-operation and readjustment of UFLS settings in high penetration of wind generation are presented in some literatures like [6] and [7], current definition of UFLS does not cover frequency support provided by inertia-less generation units in de-loaded operation.

A new Event-Based Under-Frequency Inertia Emulation (EB-UFIE) plan is proposed in this paper as a substitute of traditional UFLS program. Proposed EB-UFIE guarantees fast response to the detected high consequences disturbances for initial system protection by coordinating the fast inertia resources of the system. The developed scheme assembles a lookup table including the optimal location and amount of inertia emulation to protect the system against the risk of generation trip and subsequent blackout. To be adapted to real-time conditions of the network, the table should be updated periodically and followed by automatic timely load/generation control.

System steady state frequency succeeding a severe under-frequency condition is mainly determined by the total amount of emulated inertia through fast controllable resources, rather than their locations. However, emulating inertia in different locations alters system dynamics after UFLS action. Moreover, the cost of emulating inertia of the same amount may not be the equal at different locations. On the other hand, load feeder may be converted to a source feeder by injection of active power to the grid after emulating inertia which could not be considered in existing UFLS schemes [8]. In the proposed EB-UFIE plan, by considering the effect of the emulated inertia of these resources in frequency trajectory enhancement, interruption of useful power producer feeders are automatically avoided. The impact

of location and amount of emulated inertia are considered in the optimization model using trajectory sensitivities in order to modify the system frequency, if any under frequency time limit is violated by minimum cost.

The paper is organized as follows. Section II reviews briefly different resources of inertial response through inertia-less generation and load units. Trajectory sensitivity analysis and formulation of EB-UFEI optimization model is introduced in Section III. Section IV, contains the results of the proposed EB-UFEI plan. Concluding remarks and future works are provided in Section V.

## II. CHARACTERISTICS OF INERTIA RESOURCES

Fast resources of inertia response in power system can be generally divided into two main controllable and non-controllable categories. While the inertia produced by kinetic energy of synchronous generators and non-interruptible loads could not be controlled, demand-side controllable resources, wind and PV power plants, Electric Vehicles (EV), Multi-Terminal DC (MTDC) systems and fast-response energy storage systems could be controlled centrally or in a decentralized/distributed manner in order to provide Fast Frequency Response (FFR).

There has been numerous studies to investigate the integration of full Converter Control-Based Generators (CCBGs) in primary and secondary frequency control of power system [9], [10], [11]. Several transmission system operators have announced new grid codes requiring wind turbines and PVs to provide frequency response. The model and technical constraint and parameters of different inertia resources should be incorporated in the optimization model of UFLS. In [1], [12], [13] several inertia and frequency control techniques such as hidden inertia emulation, de-loading, droop control and fast power reserve are reviewed for variable speed wind turbines and solar PV generators. A systematic method for controlling an energy storage system for preventing load shedding due to transient declines in frequency is proposed and evaluated in [14]. National Grid is creating a new internationally leading service to take advantage of the fast response capability of storages named Enhanced Frequency Response (EFR) [15]-[16]. It should be mentioned that new service markets will need to be designed to take advantage of these inertia resources capabilities. The cost of provided inertia through inertia-less generation units should be determined through this market mechanism.

Applying an appropriate electrical torque on the rotor of the wind turbine based on the measured Rate of Change of Frequency (RoCoF) of system releases kinetic energy from the blades and the rotor. This slows the rotor which in turn the kinetic energy stored in the rotating wind turbine blades will be released a similar fashion to a synchronous generator [17], [18]. The frequency model is shown as follows [19]:

$$\Delta f_{\omega} = \frac{\Delta P_{\omega}}{K_{\omega}} \quad K_{\omega} = \frac{-1}{1+T_{\omega}s} \times \frac{1}{s} \times \frac{dp}{d\omega} \quad (1)$$

where  $K_{\omega}$  and  $T_{\omega}$  are frequency characteristic constant and a time constant of inertia controller, respectively. Blade angle

pitch control scheme is also required in order to generate power reserve by working in a de-loading state.

In case of PV units, inertial response is not related to the natural behavior of plant because no rotating part is involved. A control structure should be designed to respond in the same time frame of the classical inertia response of conventional units in de-loaded operation [20]-[21]. The frequency model of the related controller is similar to the frequency model presented in (1).

The frequency response of storage can be similar to conventional units when participating in inertia response. When the system is faced with large amount of power deficiency, ESS can provide FFR based on the following transfer function [22]:

$$\Delta f_e = \frac{\Delta P_e}{K_e} \quad K_{\omega} = \frac{-(k_{df}s+k_{pf})}{1+T_e s} \quad (2)$$

where  $k_{df}$  and  $k_{pf}$  are inertia constant and primary frequency constant of control, respectively, and consistent with conventional units.  $T_e$  is the time constant of ESS. By adding ESS to a PV unit or wind farm inertial response control of the grid could be improved. Other resources of inertia could be integrated with the proposed EB-UFEI scheme. As the time response of the CCBGs for inertia emulation are similar to conventional units, the change in their output could be controlled as a constant multiples of RoCoF by a supervisor in a centralized control manner.

## III. MATHEMATICAL MODEL OF EB-UFEI

A EB-UFEI program is well-designed if minimizes economic loss while satisfying both the steady state and dynamic criteria containing max permissible RoCoF, Nadir frequency and quasi steady state frequency by considering the actual system characteristics and the disturbance situations. Dynamics of rotor swing, governor action, load damping, location of inertia emulation, shedding location, generation and system under-frequency time limits, and RoCoF relays of DGs should be considered in an ideal EB-UFEI design.

The control signals of inertia emulation are obtained by solving mixed-integer programming problems. System dynamics in EB-UFEI will be approximated with discrete linear constraints based on trajectory sensitivity analysis which has been used in several papers to consider system dynamic in optimization process and predict the future behavior of the system [23]-[24]. Large disturbance behavior of power systems are integrated into the optimization model by linearization around a nonlinear trajectory.

EB-UFEI determines the optimal emulated inertia solutions for each severe disturbance to satisfy system performance criteria. Performance requirements for frequency dynamics are imposed within the constraints using trajectory sensitivities and based on system and generators frequency and time limits.

### A. Trajectory sensitivities

Behavior of large disturbance around a nonlinear and non-smooth trajectory can be linearized to form the first order estimation in time domain using trajectory sensitivities in which

the influence of parameter variations on large disturbance behavior are calculated. The applications of trajectory sensitivity analysis in power systems are summarized in [25].

Following set of nonlinear Differential-Algebraic Equations (DAEs) represents a power system as a function of  $x$ ,  $y$ , and  $\lambda$  which are vectors of state (e.g. rotor angle and frequency), algebraic (e.g. voltages and power), and control (e.g. load and control parameters of inertia resources) variables. By solving these equations the time-varying trajectories of state variables  $x$  are calculated.

$$\dot{x} = F(x, y, \lambda) \quad 0 = G(x, y, \lambda) \quad (3)$$

$\lambda$  is a parameter describing for example, load, generation, transmission line impedance or generator bus initial voltage levels, which is expected to change and affect the operating boundary imposed by dynamic constraints. To study the impact of emulated inertia on the system frequency, trajectory sensitivities are calculated by taking the first derivatives of the DAE (1)-(2) with respect to  $\lambda$ , as sensitivity equations [22]:

$$\dot{x}_\lambda = F_x \frac{\partial x}{\partial \lambda} + F_y \frac{\partial y}{\partial \lambda} + F_\lambda \quad 0 = G_x \frac{\partial x}{\partial \lambda} + G_y \frac{\partial y}{\partial \lambda} + G_\lambda \quad (4)$$

The continuous form of Center of Inertia (CoI) swing equation presented in (5) is linearized as (6).

$$\frac{2H}{f_0} \frac{df(t)}{dt} = \sum_{i=1}^{N_g} P_{mi} - P_{ei} \quad (5)$$

$$\frac{d\Delta f(t)}{dt} = \frac{f_0}{2H} \Delta P^{im}(t) \quad (6)$$

$$\Delta P^{im}(t) = \Delta P^{gov}(t) - \Delta P^c(t) + \Delta P^{sh}(t) + \Delta P^{wind}(t) + \Delta P^{PV}(t) + \Delta P^{ESS}(t) - D\Delta f(t)$$

Generation and load changes which may cause input power imbalance are: Generation outage ( $\Delta P^c$ ), Governor action ( $\Delta P^{gov}$ ), Wind, PV, and ESS inertia response ( $\Delta P^{wind}$ ,  $\Delta P^{PV}(t)$ ,  $\Delta P^{ESS}(t)$ ) and load changes is incurred by load shedding ( $\Delta P^{sh}(t)$ ), and load damping ( $D\Delta f(t)$ ). By assuming each term of  $\Delta P^{im}$  as  $X$ , the system frequency response is discretized over time with time step  $\Delta t$  as  $\Delta X(n\Delta t) = \Delta X_n$ .

$$\Delta f_{n+1} = \Delta f_n + \Delta t \frac{f_0}{2H} (\Delta P_n^{gov} - \Delta P_n^c + \Delta P_n^{sh} + \Delta P_n^{wind} + \Delta P_n^{PV} + \Delta P_n^{ESS} - D\Delta f_n)$$

$$\Delta P_{n+1}^{gov} = \Delta P_n^{gov} + \frac{-\Delta t}{T} (\Delta P_n^{gov} + \frac{\Delta f_n}{R}) \quad (7)$$

In this paper, by assuming  $EI$  (the amount of Emulated Inertia by loads and CCBGs) as parameter  $\lambda$  and simulating the system model for two different values of  $EI$  ( $EI$  and  $EI+\Delta EI$ ) and using the following equations, discretized frequency trajectory and relevant sensitivities are approximated. By using this method, the influence of all frequency-dependent terms of  $\Delta P^{im}$  are considered in the approximation of sensitivities through simulations.

$$\frac{\partial f}{\partial EI}(t) = \lim_{\Delta EI \rightarrow 0} \left( \frac{f(t)|_{EI+\Delta EI} - f(t)|_{EI}}{\Delta EI} \right) \approx \frac{f(t)|_{EI+\Delta EI} - f(t)|_{EI}}{\Delta EI}$$

$$f(t) = f^{base}(t) + \Delta f(t)$$

$$f(t) \approx f^{base}(t) + \frac{\partial f}{\partial EI}(t) \Delta EI \quad (8)$$

(8) will be used as frequency dynamic constraints in EB-UFIE optimization model.

### B. EB-UFIE Formulation

Optimal inertia emulating and load shedding solutions for each severe disturbance is determined by EB-UFIE to achieve system and generators performance criteria. Performance requirements for frequency dynamics are imposed within the EB-UFIE constraints. The formulation of EB-UFIE that determines the optimal solution is as follows:

$$\text{Min. CF} = \sum_{i=1}^I \Delta EI_i \times IC_i \quad (9)$$

subject to

Transient and steady state frequency approximation:

$$f(k) = f_{base}(k) + \sum_{i=1}^I \frac{\partial f}{\partial EI_i}(k) \Delta EI_i$$

Linearized under-frequency time limits:

$$\frac{f_d - f(k)}{M} < u_d(k) < \frac{f_d - f(k)}{M} + 1$$

$$0 < r_d(k-1) \leq u_d(k-1). B$$

$$T_d(k) = r_d(k-1) + u_d(k-1). \Delta t(k-1)$$

$$0 < T_d(k-1) - r_d(k-1) \leq [1 - u_d(k-1)]. B$$

$$T_d(k) \leq T_{d,max}$$

Reference frequency constraints:

$$f_{ref} - \Delta f_{ref} < f_{st,base} + \sum_{i=1}^I \frac{\partial f_{st}}{\partial EI_i} \Delta EI_i < f_{ref} + \Delta f_{ref}$$

Inertia emulating constraints:

$$0 < \Delta EI_i \leq \Delta EI_{i,max}$$

$k$ : time-series index of discretized trajectory

$i$ : index of inertia resources

$f_d$  and  $T_d, T_{d,max}$ : Frequency and time duration and limit  $d$

$M, B$ : Large positive value

$IC$ : Inertia Cost

$u_d, r_d$ : Binary and integer variable

In this studies, it is assumed that the time limit for system frequency less than 48.5 Hz is zero and the quasi-steady state frequency (acceptable for 10 sec at before full activation of primary frequency response) should be greater than 49 Hz. Also,

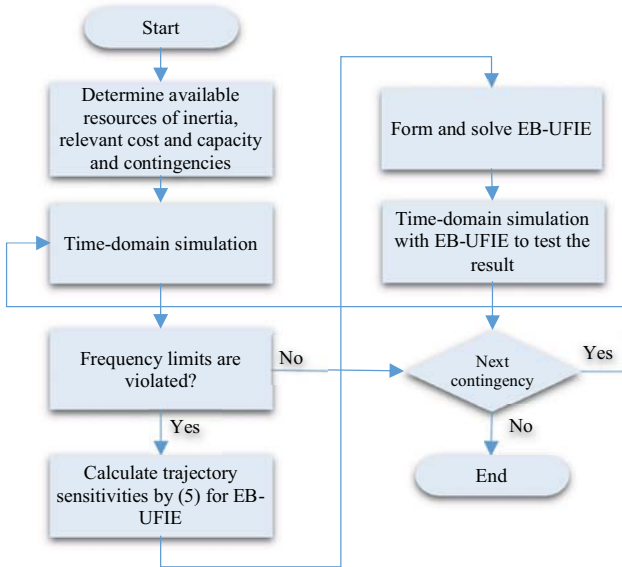


Fig. 1. Flowchart of EB-UFIE scheme implementation.

steady state frequency should reach at least 49.5 Hz. Flowchart of proposed EB-UFIE scheme implementation is shown in Fig. 1. Any other under-frequency time limits are applicable to the proposed EB-UFIE optimization

#### IV. CASE STUDY

The MATLAB and DigSILENT simulation platforms provides an efficient way to run the time-domain simulation, calculate trajectory sensitivities, and optimize the proposed mixed integer linear programming optimization model of EB-UFIE on modified New England 39-bus system.

Schematic of the modified IEEE 39-bus New England network mentioning the modifications is shown in Fig. 2. Summary result of modified network is as follows.

Table 1. Summary result of 39-bus modified network.

Conv. Gens	CCBGs	Load	Pen%	Total Gen.	Losses
5133.27	1000	6097.1	16.30	6133.27	36.17

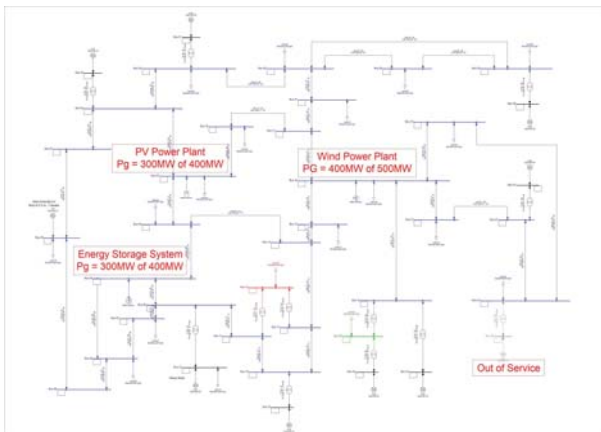


Fig. 2. Schematic of the modified IEEE 39-bus New England network.

EB-UFIE is implemented on the modified IEEE 39-bus test system based on the presented flowchart in Fig. 1.

#### A. Time-domain simulation and trajectory sensitivities

DigSILENT Power Factory is used in order to simulate system model in different contingencies in base case in order to find the violated under-frequency time limits. G01 and G09 are recognized as most severe contingencies as shown in Fig. 3. In both disturbances, all the under\*frequency limits are despoiled.

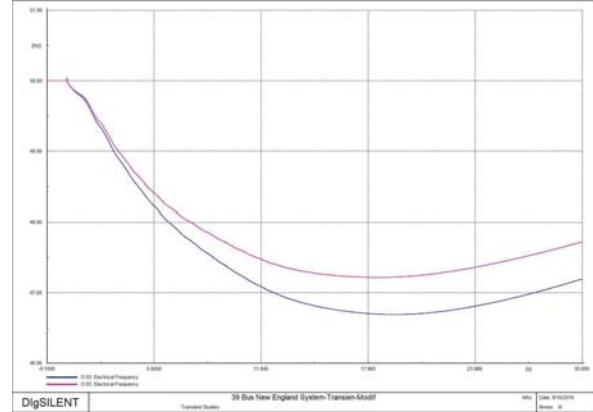


Fig. 3. Frequency in outage of G01 (blue) and in outage of G09 (pink).

By applying a slight change e.g.  $10\%P_{nom}$  or 0.1 p.u. in each resource of inertia including all loads and three CCBGs, the affected frequency trajectories are obtained. Using (8), frequency trajectory sensitivities are calculated in each time-series index of discretized trajectory assuming 50ms as time step. In Fig. 4, the G03 frequency trajectory is presented in outage of G01 at  $t = 1.0$  sec. Through the reaction of wind power plant to the contingency after 200msec and in scale of 0.1 p.u. the frequency is improved. The difference between frequencies of two trajectories (base and affected one) in each time step divided by 0.1 p.u. or  $10\%P_{nom}$  provides trajectory sensitivities and thereupon, discretized transient and steady state frequency approximation.

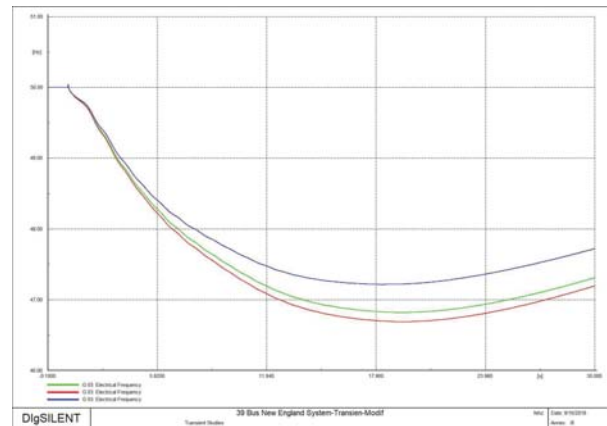


Fig. 4. Frequency path following outage of G01 (red), in case of 0.1 p.u. emulated inertia through wind plant(blue), and 10% load shedding at bus 25 (green) after 0.2sec delay.

### B. EB-UFIE scheme and implementation

Base-case discretized frequency trajectory and calculated trajectory sensitivities with respect to a small change in shedded load and fast frequency response of CCBGs are used to formulate (9) in disturbance of G09. Inertia Cost are assumed higher in CCBGs rather than loads in order to show the trade of cost and sensitivity in optimization model and provided solution. CCBGs can provide higher Time limit for system frequency less than 48.5 Hz is assumed zero and the steady state frequency should be greater than 49.5 Hz. The optimization solution is obtained by using Genetic Algorithm which assembles a lookup table including the optimal location and amount of inertia emulation to protect the system against the risk of generation G09 trip. Time-domain simulation with EB-UFIE is down through DIgSILENT to test the result in real system.

The amount of obligatory shedding load and emulating inertia in disturbance of G09 to contain system frequency in limits are determined as 358.24 MW and 153.53 MW, respectively. The amount and location of each part is . The emulation and shedding should be fully activated 200 msec after recognition of the relevant large disturbance. Traditional UFLS plan requires 640 MW load shedding to maintain the system frequency trajectory within the transient and steady state limits.

In Fig. 5, the system frequency trajectory modified through the EB-UFIE look-up table (red) in disturbance of G09 is presented. The system frequency in base case is also shown in blue.

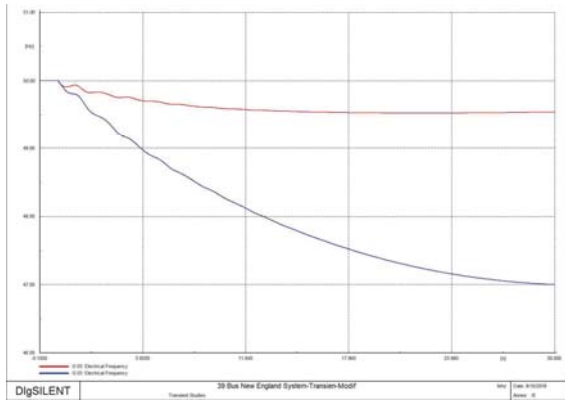


Fig. 5. Frequency path following outage of G01 (red), in case of 0.1 p.u. emulated inertia through wind plant(blue), and 10% load shedding at bus 25 (green) after 0.2sec delay.

Different sensitivities could also be integrated into the EB-UFIE optimization model such as voltage sensitivities and voltage trajectory.

### V. CONCLUSION AND FUTURE WORKS

This paper has presented an inertia control scheme for severe disturbances through an EB-UFIE mixed integer programming optimization problem modelling coordinating wide-area inertial resources. Trajectory sensitivities incorporate the frequency trajectory variations with the change of inertia for better computational efficiency. The EB-UFLS guarantees fast response to severe under-frequency conditions to maintain

system stability with minimum time delay. New service markets could be designed to take advantage of these inertia resources capabilities.

The estimation of disturbances and inertia emulation process could be more inter-connected in real time operation due to more accessibility of power system state information through the recent development of the Supervisory Control and Data Acquisition (SCADA) system and the Wide Area Measurement (WAM) system and using high performance computers. It also could be controlled in distributed manner rather than central control which delays reaction of inertia resources to the disturbances. This assumption might be addressed in future studies.

### ACKNOWLEDGMENT

This work was partially supported by the European Commission under project FLEXITRANSTORE — H2020-LCE-2016-2017-SGS-774407 and by the Spanish Ministry of Science under project ENE2017-88889-C2-1-R. Any opinions, findings and conclusions or recommendations expressed in this material are those of the authors and do not necessarily reflect those of the host institutions or funders.

### REFERENCES

- [1] M. Dreidy, H. Mokhlis, and S. Mekhilef, "Inertia response and frequency control techniques for renewable energy sources: A review," *Renew. Sustain. Energy Rev.*, vol. 69, no. November 2015, pp. 144–155, 2017.
- [2] P. Rodriguez, C. Citro, J. I. Candela, J. Rocabert, and A. Luna, "Flexible Grid Connection and Islanding of SPC-Based PV Power Converters," *IEEE Trans. Ind. Appl.*, vol. 54, no. 3, pp. 2690–2702, 2018.
- [3] S. D'Arco, J. A. Suul, and O. B. Fosfo, "A Virtual Synchronous Machine implementation for distributed control of power converters in SmartGrids," *Electr. Power Syst. Res.*, vol. 122, pp. 180–197, 2015.
- [4] J. Morren, S. W. H. de Haan, W. L. Kling, and J. A. Ferreira, "Wind Turbines Emulating Inertia and Supporting Primary Frequency Control," *IEEE Trans. Power Syst.*, vol. 21, no. 1, pp. 433–434, 2006.
- [5] L. Tang and J. McCalley, "Two-stage load control for severe under-frequency conditions," *IEEE Trans. Power Syst.*, vol. 31, no. 3, pp. 1943–1953, 2016.
- [6] F. Gonzalez-Longatt, J. Rueda, and E. Vázquez Martínez, "Effect of Fast Acting Power Controller of Battery Energy Storage Systems in the Under-frequency Load Shedding Scheme," *International Conf. Innov. Smart Grid Technol. (ISGT Asia 2018)*, no. June, 2018.
- [7] N. Aparicio, S. Añó-Villalba, E. Belenguer, and R. Blasco-Gimenez, "Automatic under-frequency load shedding mal-operation in power systems with high wind power penetration," *Math. Comput. Simul.*, vol. 146, no. 2017, pp. 200–209, 2018.
- [8] B. Hoseinzadeh, F. F. Da Silva, and C. L. Bak, "Decentralized Coordination of Load Shedding and Plant Protection Considering High Share of RESs," *IEEE Trans. Power Syst.*, vol. 31, no. 5, pp. 3607–3615, 2016.

- [9] M. Raju, L. C. Saikia, and N. Sinha, "Load frequency control of multi-area hybrid power system using symbiotic organisms search optimized two degree of freedom controller," *Int. J. Renew. Energy Res.*, vol. 7, no. 4, pp. 1664–1674, 2017.
- [10] A. J. Veronica and N. S. Kumar, "Internal Model Based Load Frequency Controller Design for Hybrid Microgrid System," *Int. J. Renew. Energy Res.*, vol. 7, no. 2, pp. 778–786, 2017.
- [11] J. Patino, F. Valencia, and J. Espinosa, "Sensitivity Analysis for Frequency Regulation in a Two-Area Power System," *Int. J. Renew. Energy Res.*, vol. 7, no. 2, pp. 700–706, 2017.
- [12] M. Abdollahi, J. Ignacio Candela, J. Rocabert, R. S. M. Aguilar, and P. Rodriguez, "Generation frequency support by renewable SSG SPC unit on interconnected areas," *2017 6th Int. Conf. Renew. Energy Res. Appl. ICRERA 2017*, vol. 2017–Janua, pp. 977–982, 2017.
- [13] S. M. Vaca, C. Patsios, and P. Taylor, "Enhancing frequency response of wind farms using hybrid energy storage systems," *2016 IEEE Int. Conf. Renew. Energy Res. Appl.*, vol. 5, pp. 325–329, 2016.
- [14] S. Pulendran, S. Member, and J. E. Tate, "Energy Storage System Control for Prevention of Transient Under-Frequency Load Shedding," pp. 1–11, 2015.
- [15] D. M. Greenwood, K. Y. Lim, C. Patsios, P. F. Lyons, Y. S. Lim, and P. C. Taylor, "Frequency response services designed for energy storage," *Applied Energy*, vol. 203, pp. 115–127, 2017.
- [16] U. Zlwk, "meeting frequency response requirement with uncertain system inertia," vol. 5, pp. 5–10, 2016.
- [17] E. Ørum, M. Laasonen, and et al, "Future system inertia," pp. 1–58, 2015.
- [18] H. R. Chamorro *et al.*, "Distributed Synthetic Inertia Control in Power Systems," *Proc. 8th Int. Conf. Energy Environ. Energy Saved Today is Asset Futur. CIEM 2017*, pp. 74–78, 2018.
- [19] H. Li, J. Wang, Z. Du, F. Zhao, H. Liang, and B. Zhou, "Frequency control framework of power system with high wind penetration considering demand response and energy storage," no. October, pp. 19–20, 2017.
- [20] C. Rahmann and A. Castillo, "Fast frequency response capability of photovoltaic power plants: The necessity of new grid requirements and definitions," *Energies*, vol. 7, no. 10, pp. 6306–6322, 2014.
- [21] A. K. V. D. and P. K., "Recent Advances and Control Techniques in Grid Connected Pv System – A Review," *Int. J. Renew. Energy Res.*, vol. 6, no. 3, pp. 1037–1049, 2016.
- [22] J. Khazaei, D. H. Nguyen, and N. G. M. Thao, "Primary and secondary voltage/frequency controller design for energy storage devices using consensus theory," *2017 6th Int. Conf. Renew. Energy Res. Appl. ICRERA 2017*, vol. 2017–Janua, 2017.
- [23] I. a. Hiskens and M. a. Pai, "Trajectory sensitivity analysis of hybrid systems," *IEEE Trans. Circuits Syst. I Fundam. Theory Appl.*, vol. 47, no. 2, pp. 204–220, 2000.
- [24] I. a. Hiskens and M. a. Pai, "Power system applications of trajectory sensitivities," *2002 IEEE Power Eng. Soc. Winter Meet. Conf. Proc. (Cat. No. 02CH37309)*, vol. 2, no. 4, pp. 1–6, 2002.
- [25] L. Tang and W. Sun, "An Automated Transient Stability Constrained Optimal Power Flow Based on Trajectory Sensitivity Analysis," *IEEE Trans. Power Syst.*, vol. 32, no. 1, pp. 590–599, 2017.